Chapter 7

Oxidation of Glycerol to Lactic Acid by Gold on Acidified Alumina: A Kinetic and DFT Case Study

Thabang A. Ntho, Pumeza Gqogqa and James L. Aluha

Additional information is available at the end of the chapter

http://dx.doi.org/10.5772/intechopen.70485

Abstract

The aim of this chapter is to present proposed kinetic and density functional theory (DFT) models for the selective oxidation of glycerol to various hydroxy-acids over an acidified Au/γ-Al_2O_3 catalyst. Glycerol oxidation over gold-based catalysts to value-added chemicals continues to attract attention worldwide. Both the kinetics and theoretical mechanisms of this reaction have been reported in the past. However, some of the reported kinetic data was possibly collected under mass transfer limitations. In this case study we demonstrate that if mass transfer is eliminated, a pseudo zero-order model can be fitted to the experimental data with a high degree of correlation. Furthermore, we propose a plausible mechanism of pyruvaldehyde (PA) isomerisation to lactic acid (LAC) over supported molybdenum Lewis acid sites as investigated with density functional theory (DFT) approach. A proposed DFT model suggested that the rate-limiting step in the isomerisation of PA to LAC, catalysed by a Mo Lewis acid-site, could be the dissociation of a proton from an adsorbed water molecule – the protonation step.

Keywords: gold, catalyst, alumina, support-acidity, glycerol-oxidation, lactic acid, kinetics, DFT

1. Introduction

Lactic acid (LAC), as noted by Wee et al. [1], is one of the most valuable chemicals in industry today and is widely used in the food, cosmetic, pharmaceutical, and chemical industries. In the food industry, for example, it may be used as a preservative, an acidulant, or for flavouring, while in the textile, pharmaceutical and chemical industry it is used as a raw material for the production of lactate ester, propylene glycol, 2,3-pentanedione, propanoic acid, acrylic acid,

acetaldehyde and dilactide. In fact, LAC continues to receive increased attention for its potential use as a monomer in the production of biodegradable poly lactic acid. It can be produced by either biotechnological fermentation or chemical synthesis, but the former route is receiving considerable interest due to environmental concerns and the limited nature of petrochemical feedstocks. However, fermentation is inherently a slow process. An alternative route to LAC is by processing a 'renewable' resource such as glycerol by means of heterogeneous catalysis. Haruta [2] has reported that gold with particle diameters below 10 nm are surprisingly active for many reactions, such as CO oxidation and propylene epoxidation.

Many aspects of glycerol oxidation by Au have been studied. Ketchie et al. [3] have looked at the effect of Au particle size, particularly on supports such as carbon [4] and titania [5], while Wang et al. [6] have examined the effect of particle shape, and Villa et al. [7] have investigated the role of stabilizers in gold sols as catalysts in the liquid-phase oxidation of glycerol. In addition, Demirel et al. [8] have probed the promotional effect of Pt on Au/C catalysts, and Royker et al. [9] have investigated the promotional effect of Pt on Au/Al_2O_3 catalysts, while other authors have studied the effect of base in the reaction. For example, Chornaja et al. [10] examined the oxidation of glycerol to glyceric acid using Pd catalysts that worked in alkaline media, and Ketchie et al. [5] reported the promotional effect of hydroxyl ions over Au catalysts, while Carretin et al. [11] have analysed the effect of base as a reaction initiator, proving that for Au/C catalysts, the presence of OH^- was mandatory for any meaningful glycerol oxidation to occur. However, there was seemingly very limited study on the effect of surface acidity for this reaction using alumina supports, for which this work is dedicated.

2. Experimental procedures

2.1. Chemical reagents and materials

Commercial γ-Al_2O_3 support (denoted as Degussa 2010, BET specific surface area of 260 $m^2\ g^{-1}$), ammonium molybdate $(NH_4)_6{\cdot}Mo_7O_{24}{\cdot}4H_2O$ from Associated Chemical Enterprises (ACE), chloroauric acid $HAuCl_4{\cdot}3H_2O$ from Rand Refinery (South Africa), NaOH (98%) and nitric acid (65%) from ACE, and glycerol (99.5%) from Rochelle Chemicals were used.

2.2. Preparation of MoO_3/γ-Al_2O_3 support

A mass of 4.6 g of γ-Al_2O_3 support with a measured BET specific surface area of 245 $m^2\ g^{-1}$ was weighed and placed in a beaker. About 100 ml solution of 0.1 M ammonium molybdate salt was measured, enough to form MoO_3 monolayer coverage at surface concentration of 5 atoms of metal nm^{-2} or 0.2 $nm^2\ atom^{-1}$ according to Stobbe-Kreemers et al. [12] and Raubenheimer and Cronje [13]. The pH of the solution was then adjusted to a value below 1 by addition of dilute (0.25 M) HNO_3 acid, with agitation to ensure equal distribution of the acid to a stable pH. The support was then added to the ammonium molybdate solution and left to stand for 8 h, after which, it was filtered and left to oven dry in air at 120°C for 16 h. The dried catalyst precursor was then calcined in air at a flow rate of 300 SCCM at 500°C for 4 h to decompose any residual ammonium and nitrate ions from the support, effectively reducing the molybdate ion to MoO_3,

thereby anchoring it to the alumina support. Gold was loaded onto the supports as described elsewhere [14].

2.3. Catalyst testing conditions

Catalyst testing for glycerol oxidation was performed at 90°C (with temperature optimised at 60 and 90°C) and oxygen pressure kept at 8.5 bar using a glass-lined Parr reactor (model 4563), in batch mode under agitation with stirrer speed kept constant at 1000 rpm, using 0.5 g of catalyst for 10 g of glycerol dissolved in 90 g of de-ionized water. To this solution, NaOH pellets were added such that the mole ratio of glycerol to the base was always 1:2. In-depth details are provided elsewhere [14].

2.4. Catalyst characterisation

2.4.1. High resolution transmission electron microscopy (HRTEM)

HRTEM analysis was conducted on a field emission microscope, the JEM2100F electron microscope from JEOL Ltd., fitted with energy-dispersive X-ray spectroscopy (EDX), wavelength dispersive spectroscopy (WDS) and electron beam backscattered diffraction (EBSD) operating on Oxford Instruments software. The instrument was operated at an accelerating electron beam of 200 kV and images captured in the bright field mode. The Nano-measurer 1.2 'Scion Imager' software was used for particle size analysis.

2.4.2. Temperature programmed desorption (TPD)

The acidity of the materials was qualitatively measured by temperature programmed desorption (TPD) of NH_3 on a micromeritics automated catalyst characterisation system: model AutoChem II 2920 chemisorption analyser. NH_3-TPD studies were performed by loading 0.25 g catalyst in a U-tube reactor and cleaning the sample in a gas stream of helium at 120°C for an hour at a ramping rate of 10°C min^{-1} to remove moisture and other adsorbed species. A mixture of 10% NH_3 balanced in He was flushed over the sample isothermally at 120°C. After adsorption was achieved at 120°C, the NH_3 desorption measurements ensued at 120°C using the thermo-conductivity detector (TCD) and data collected up to 500°C at a ramping rate of 15°C min^{-1}.

2.5. Models and computational methods

2.5.1. Kinetic parameter estimation

The regression analysis of the experimental data was performed by use of Easy Regression Analysis (ERA 3.0) software [15, 16]. The software uses the sum of the square of residual deviations as the objective function. All the kinetic parameters were estimated at a 95% confidence limit using a modified adaptive random search algorithm.

2.5.2. DFT methodology

Unless otherwise stated, all electronic energies of reactants, products and transition states were determined by density functional theory (DFT) using the $DMol^3$ code [17, 18] within the

BIOVIA Materials Studio 2016 environment using the generalised gradient approximation (GGA), with a double numerical basis set (DNP) and the Perdew-Becker-Ernzerhof (PBE) exchange-correlation functional. All electrons were included in the calculations with unrestricted spin-polarization. A fine integration grid was used together with a Fermi smearing of 0.005 Hartree (Ha). The energy convergence tolerance was set to 1.0×10^{-5} Ha; the maximum force was 0.002 Ha/Å and maximum displacement was set at 0.005 Å. The self-consistent field (SCF) density convergence was set $1.0e-6$.

The complete linear synchronous transit and quadratic synchronous transit (LST/QST) method [19] was used to locate the transition state structures according to the optimised structures of reactants and products. The nudged elastic band (NEB) method [20], as implemented in DMol^3, was used to confirm that the transition state structures lead to the expected reactant and product molecular structures. Frequency calculations were performed to confirm the nature of all stationary points as either minima or transition states (TSs).

When investigating a reaction that takes place on the surface of a heterogeneous catalyst by quantum chemical methods, one of the main difficulties is modelling an infinite catalyst system as highlighted by Handzlik and Ogonowski [21], and a viable approach with the capacity of solving this problem is by the application of cluster models. Song et al. [22] claim that, ideally, cluster models are appropriate if a suitable boundary condition is obtained such that charges are in reasonable distribution on the surface. In this study, we chose a Al_3MoO_7H cluster to represent an active site of Mo on MoO_3/γ-Al_2O_3. Assuming that the oxidation states of the elements in the model are distributed as follows: Al = 3^+, Mo = 4^+, H = 1^+ and O = 2^-; then the overall charge of the cluster would be zero. From this point of view it can be assumed that when the substrate adsorbs on Al_3MoO_7H, it occupies the vacant sites on Mo to form a cluster model in which the Mo is in an approximate octahedral environment with a 6^+ oxidation state. This adsorption mode is consistent with the work of Kong et al. [23] who indicated how LAC could be formed from adsorbed intermediates such as pyruvaldehyde (PA).

3. Results

3.1. Catalyst characterisation

The sample of the NH_3-TPD profiles is displayed in **Figure 1** shows that the Au-MoO_3/γ-Al_2O_3 catalyst was more acidic than the original γ-Al_2O_3 support. All the materials displayed noticeable Lewis acidity (that is, electron accepting sites as opposed to the Brønsted acidity, which are regarded as proton donating sites) since the ammonia desorption occurred at the lower temperatures (below 300°C). The γ-Al_2O_3 support indicated Lewis acidity having different strengths with the weaker sites desorbing NH_3 at about 180°C while the stronger sites desorbed NH_3 at about 300°C.

On the addition of gold, the Au/γ-Al_2O_3 catalyst showed a shift in the two peaks to the higher temperatures, that is, 220 and 450°C, respectively. However, the addition of MoO_3 on γ-Al_2O_3 support exhibited only the (weaker) Lewis acid sites that desorbed NH_3 at the lower temperatures, peaking at 220°C. This finding is in agreement with a number of researchers who have

http://dx.doi.org/10.5772/intechopen.70485

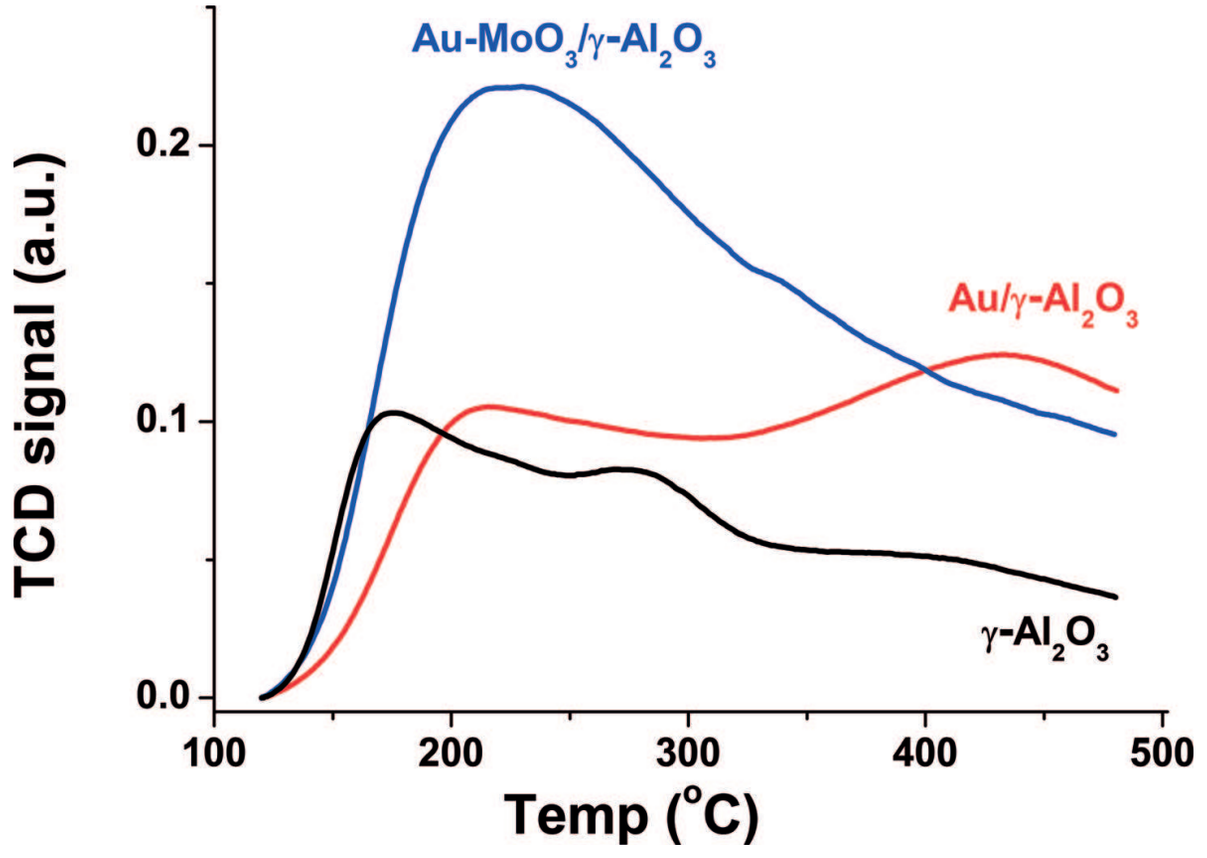

Figure 1. Qualitative analysis of the catalyst's acidity by the NH_3-TPD method.

recorded the absence of Brønsted acid sites in similar alumina systems, results which were further confirmed by their infrared studies, for example, by Lianecki et al. [24] and by XRD studies by Heracleous et al. [25]. It has been proposed by Gong et al. [26] that as long as the loading of MoO_3 on γ-Al_2O_3 is less than 16% (w/w), the nature of surface acid-base sites that exist on the surface would be predominantly of the Lewis type.

3.2. Reaction control: kinetic studies

3.2.1. The effect of base as a reaction initiator

Catalyst testing commenced with investigating the effect of NaOH as a reaction initiator on the kinetics of glycerol oxidation using Mintek's 0.9-wt% Au/γ-Al_2O_3 (AUROlite^{TM}) commercial catalyst. **Figure 2** displays a plot depicting glycerol conversion as a function of time indicating that higher base concentrations led to greater glycerol conversions thereby shortening reaction time. It has indeed been previously reported that the base acts an initiator for this reaction [5].

3.2.2. Mass transfer limitations

In order to optimise the reaction conditions for mass transfer, a number of influencing parameters, e.g. stirring speed, oxygen partial pressure, amount of catalyst and the initial

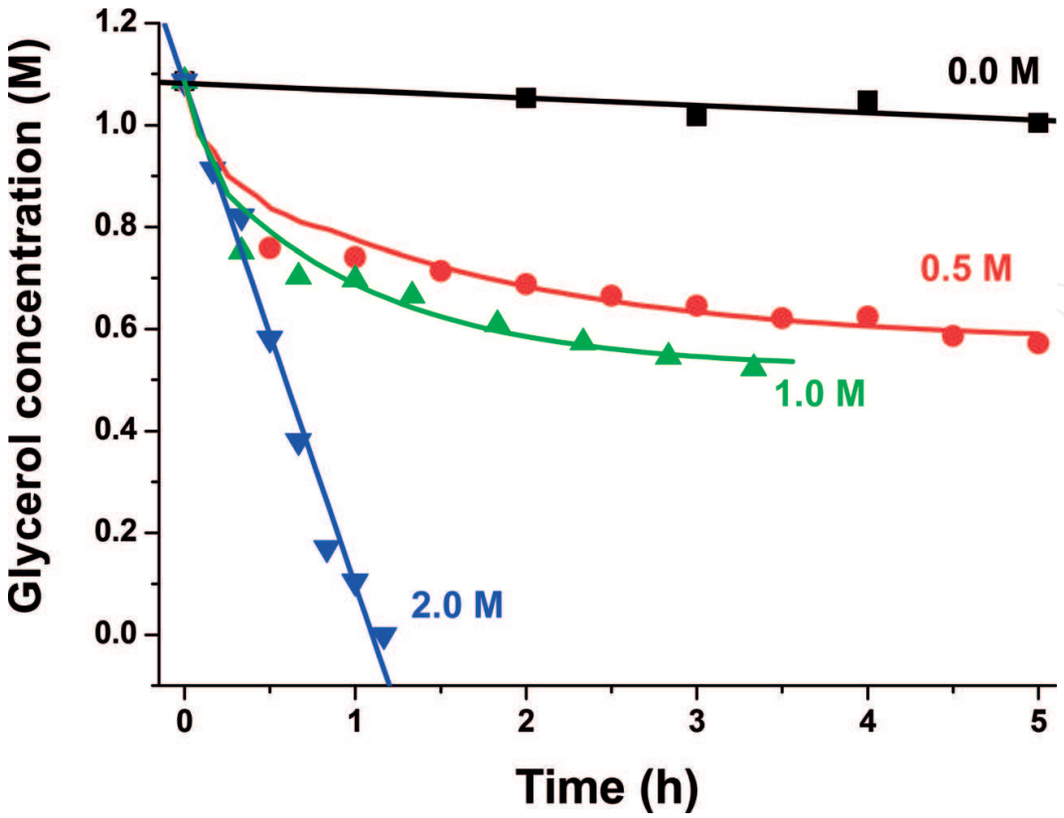

Figure 2. The effect of base concentration as a reaction initiator on glycerol oxidation using 0.5 g of 0.9-wt% Au/γ-Al_2O_3 catalyst at 90°C and O_2 pressure of 8.5 bar.

educt concentrations, were varied to arrive at the kinetic regime. The commercial 0.9-wt% Au/γ-Al_2O_3 (Aurolite^{TM}) catalyst was used to establish the mass transfer regime. The stirring rate was fixed at 1000 rpm and the amount of catalyst varied as shown in **Figure 3**. In theory, if the rate doubles with the doubling of the weight of the catalyst, then the reaction is controlled by kinetics; if this is not the case, then the reaction is controlled by mass transfer. The curve in **Figure 3** indicates that, under the defined experimental conditions, the ideal amount of catalyst necessary to achieve kinetic control was between 0.5 and 1.2 g. This 'reaction-limited' situation was ideal for the determination of intrinsic reaction kinetic parameters.

3.2.3. The effect of temperature on activation energy

In this work, the activation energy for the oxidation of glycerol over Au/γ-Al_2O_3 catalyst was experimentally determined. For a zero-order reaction, it can be shown that fractional conversion is linearly dependent on time and temperature through the relationships shown in Eq. (1) and Eq. (2):

$$X_A = \left(\frac{k}{C_{Ao}}\right) \cdot t \tag{1}$$

where X_A is the fractional conversion of reactant A,

http://dx.doi.org/10.5772/intechopen.70485

C_{A0} is the initial concentration of A,

k is the rate constant with units as mol L^{-1} min^{-1} and

t is time in minutes,

and that, k is dependent on temperature,

$$\mathbf{k} = \mathbf{A}.\mathbf{e}^{-\left(\frac{E_A}{RT}\right)} \tag{2}$$

where k is the rate constant with units as mol L^{-1} h^{-1}

A is the pre-exponential factor, specific to this reaction

E_A is the activation energy of the reaction,

R is the gas constant 8.314 J mol^{-1} K^{-1} and

T is the temperature in Kelvin.

Figure 4 shows the plot of glycerol conversion as a function of time for experiments that were carried out at 60 and 90°C. Usually, k is regarded as the rate coefficient of the overall reaction, which is some measure of catalyst activity, but in essence, as shown by Eqs. (1) and (2), k is temperature-dependent, as well as concentration-dependent, usually dependent on the initial concentration of the reactant.

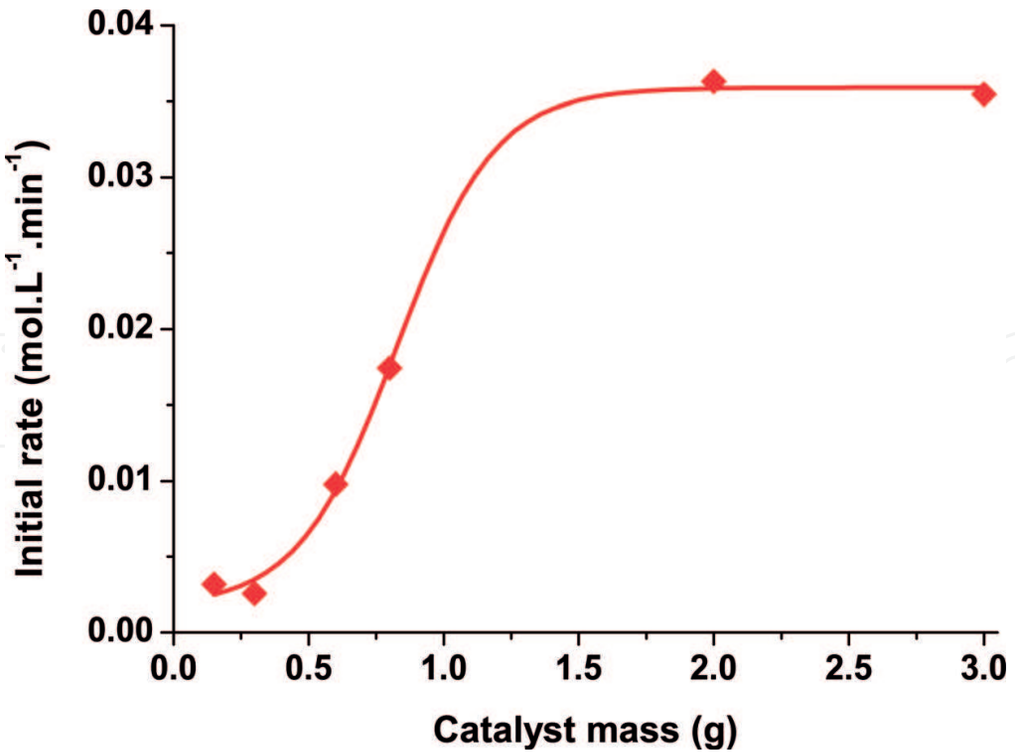

Figure 3. Initial rate as a function of catalyst mass for glycerol oxidation over 0.9-wt% Au/γ-Al_2O_3 (106–150 mμ): 1000 rpm, NaOH/glycerol = 2:1, at 60°C, under 8.5-bar O_2 pressure.

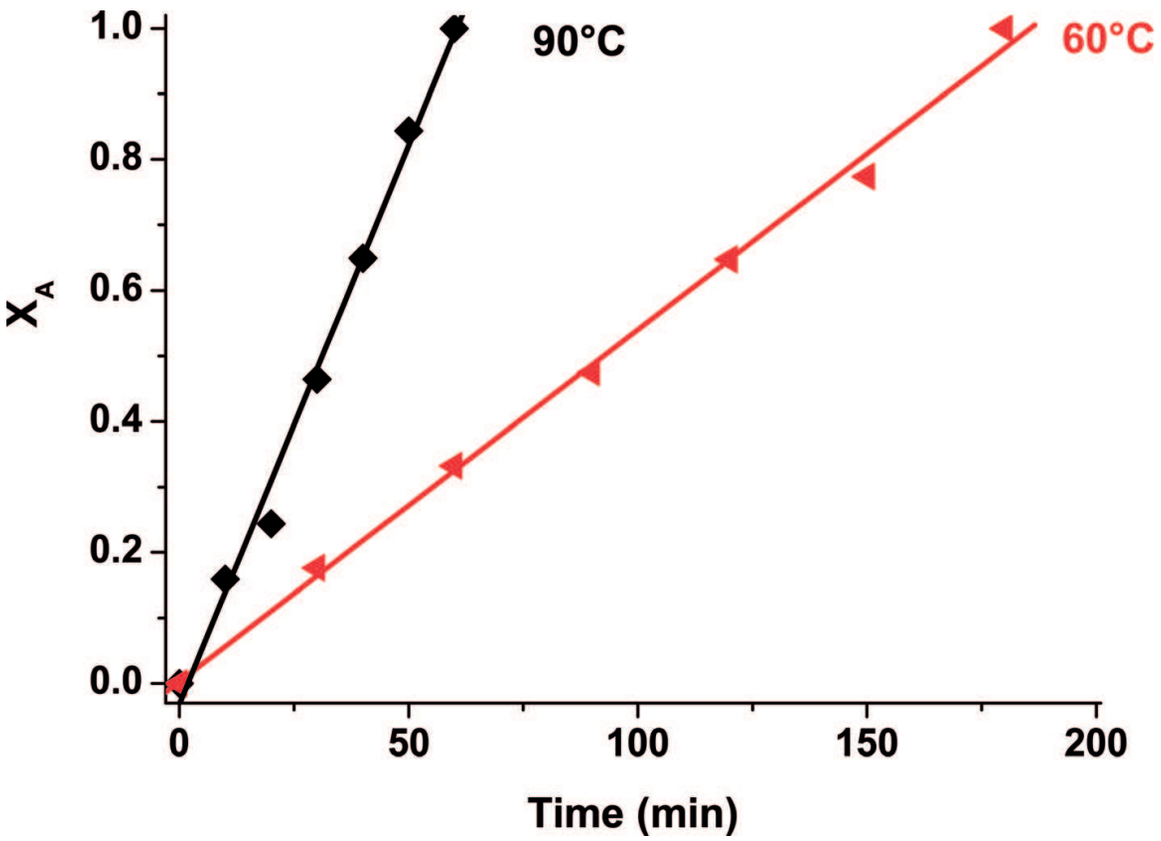

Figure 4. Conversion of glycerol over time by 0.9-wt% Au/γ-Al_2O_3 (106−150 mμ) catalyst; 1000 rpm, NaOH/glycerol = 2:1, at 60 and 90°C, under an O_2 pressure of 8.5 bar.

The rate constants, *k*, were estimated by non-linear regression of the model shown in Eq. (2) against experimental data and the results summarised in **Table 1**, showing the apparent E_A determined from the estimated rate constants using a two-point Arrhenius equation, thus:

$$E_A = \frac{T_1 \times T_2 \times R}{T_2 - T_2} ln\left(\frac{k_2}{k_1}\right) \tag{3}$$

By the use of a two-point Arrhenius equation with catalyst activity being measured at 60 and 90°C, the pre-exponential factor, *A*, was determined to be equal to 274 695 mol dm^{-3} h^{-1} under the reaction conditions employed. In addition, the *k* values for the various catalysts were determined experimentally using Eq. (2). Then, since $k = 274695.e^{-E_A/RT}$, and in substituting the values for *A* and *k* in the Arrhenius equation, the E_A per catalyst were found to be in very close proximity, with the least active catalyst (Au/γ-Al_2O_3) having the highest E_A = 37.4 kJ mol^{-1}, followed by the Au-MoO_3/γ-Al_2O_3 with E_A = 35.4 kJ mol^{-1}. The rate constants (*k*) of the catalysts for overall glycerol conversion, calculated from experimental results were observed to be 2.22 and 1.14 mol dm^{-3} h^{-1} for the Au-MoO_3/γ-Al_2O_3 and Au/γ-Al_2O_3, respectively, per gram of catalyst. Alternatively, when normalised to the amount of Au in the catalyst, the rate constants were found to be 642 mol dm^{-3} h^{-1} g_{Au}^{-1} for Au-MoO_3/γ-Al_2O_3 catalyst and 252 mol dm^{-3} h^{-1} g_{Au}^{-1} for Au/γ-Al_2O_3 catalyst.

Model[#]	Parameter	Temperature					
$X_A = \left(\frac{k}{C_{A0}}\right) \times t$	k	**60°C**			**90°C**		
		Value	**Confidence limits**		**Value**	**Confidence limits**	
		0.0059	0.0058	0.0061	0.018	0.017	0.019
$E_A = \frac{T_1 \times T_2 \times R}{T_2 - T_2} ln\left(\frac{k_2}{k_1}\right)$	E_A	**Value**			**Confidence limits**		
		37.4			36.1		38.1

Parameter values estimated at 95% confidence level; k = mol L^{-1} min^{-1} and E_A = kJ mol^{-1}.
[#]R = 8.314 J K^{-1} mol^{-1}.

Table 1. Regression analysis of conversion vs. time data for the 0.9-wt% Au/γ-Al_2O_3 catalyst at different temperatures.

The experimentally obtained E_A in this work, as shown in **Table 1**, is in good agreement with the 38 kJ mol^{-1} value reported by Wörz et al. [27] for glycerol oxidation, although their work was based on a Pt-Bi/C catalyst. Demirel et al. [28] also reported activation energies of between 40 and 50 kJ mol^{-1} for the Au/C catalysed glycerol oxidation, which is a result not far from our own. Finally, Chornaja et al. [10] also reported an apparent E_A of about 39 ± 3 kJ mol^{-1} for glycerol oxidation over Pd/Al_2O_3, which is also consistent with our findings.

As a control, both the bulk γ-Al_2O_3 and MoO_3/γ-Al_2O_3 supports did not show any activity towards glycerol oxidation at 90°C.

3.2.4. The effect of Au nanoparticle size

The effect of Au particle size on the kinetics of glycerol conversion was also investigated. **Figure 5** shows TEM images of three Au/γ-Al_2O_3 catalysts with different Au particle sizes. When screened for glycerol oxidation under the same reaction conditions, the catalysts surprisingly revealed that the kinetics of this reaction strongly depend on the metal particle size, as shown in **Figure 6**. Big Au nanoparticles, *ca* 20 nm, exhibit first-order kinetics while the data for smaller Au nanoparticles, *ca* 4 nm, does not fit this model, instead showing zero-order kinetics as it has already been discussed. More details of this phenomenon have already been reported elsewhere [14].

3.3. Global kinetic model prediction

So far we have only concentrated on the depletion kinetics of the reactant. In this section, we explore the global kinetics of the reaction, i.e. we set-up a kinetic model that takes into account the full mass balance of the reaction. At full substrate penetration and surface coverage, conversion is not limited by mass transfer; it is a fixed quantity set by the zero-order kinetics. Accordingly, mass transfer terms have not been explicitly expressed in the kinetic model used in this study since kinetic data was collected under the kinetic control regime. Therefore, **Figure 7** presents the reaction network on which the kinetic modelling was based. The concentrations of all the compounds in the figure were taken into account in the calculations. Since the partial pressure (hence concentration) of O_2 was maintained high in excess, its surface coverage

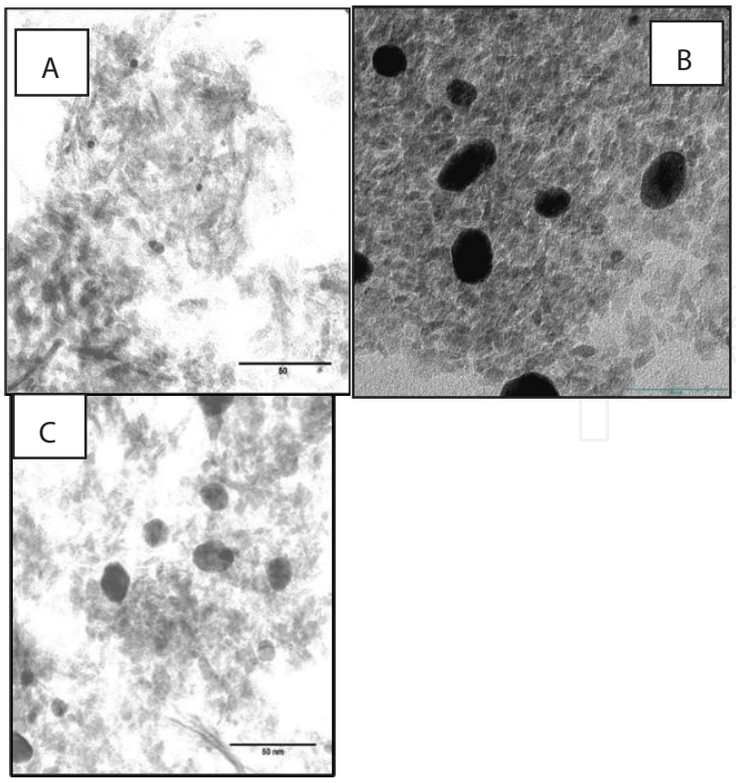

Figure 5. TEM images of Au/γ-Al_2O_3 catalysts prepared by various reducing agents: (A) reduced with 5% H_2 (~4 nm); (B) reduced with THPC (~17 nm); and (C) reduced with PVA–citrate (~21 nm). Catalyst preparation details were outlined elsewhere [14].

was assumed constant and the surface reactions were modelled as pseudo-monomolecular in the tested model.

The complete mass balance, based on **Figure 7**, is represented by Eqs. (4)–(8). The model is pseudo-zero-order overall and contains five parameters in total.

$$\frac{dC_1}{dt} = -(r1 + r3) = -k_1 \tag{4}$$

$$\frac{dC_2}{dt} = r1 - r2 = k_2 - k_3 \tag{5}$$

$$\frac{dC_3}{dt} = r2 = k_3 \tag{6}$$

$$\frac{dC_4}{dt} = r3 - r4 = k_4 - k_5 \tag{7}$$

$$\frac{dC_5}{dt} = r4 = k_5 \tag{8}$$

http://dx.doi.org/10.5772/intechopen.70485

Each rate constant, k_i, is defined as:

$$k_i = A_i e^{\frac{-E_{A_i}}{RT}} \tag{9}$$

where A_i is the frequency factor and E_{Ai} is the activation energy.

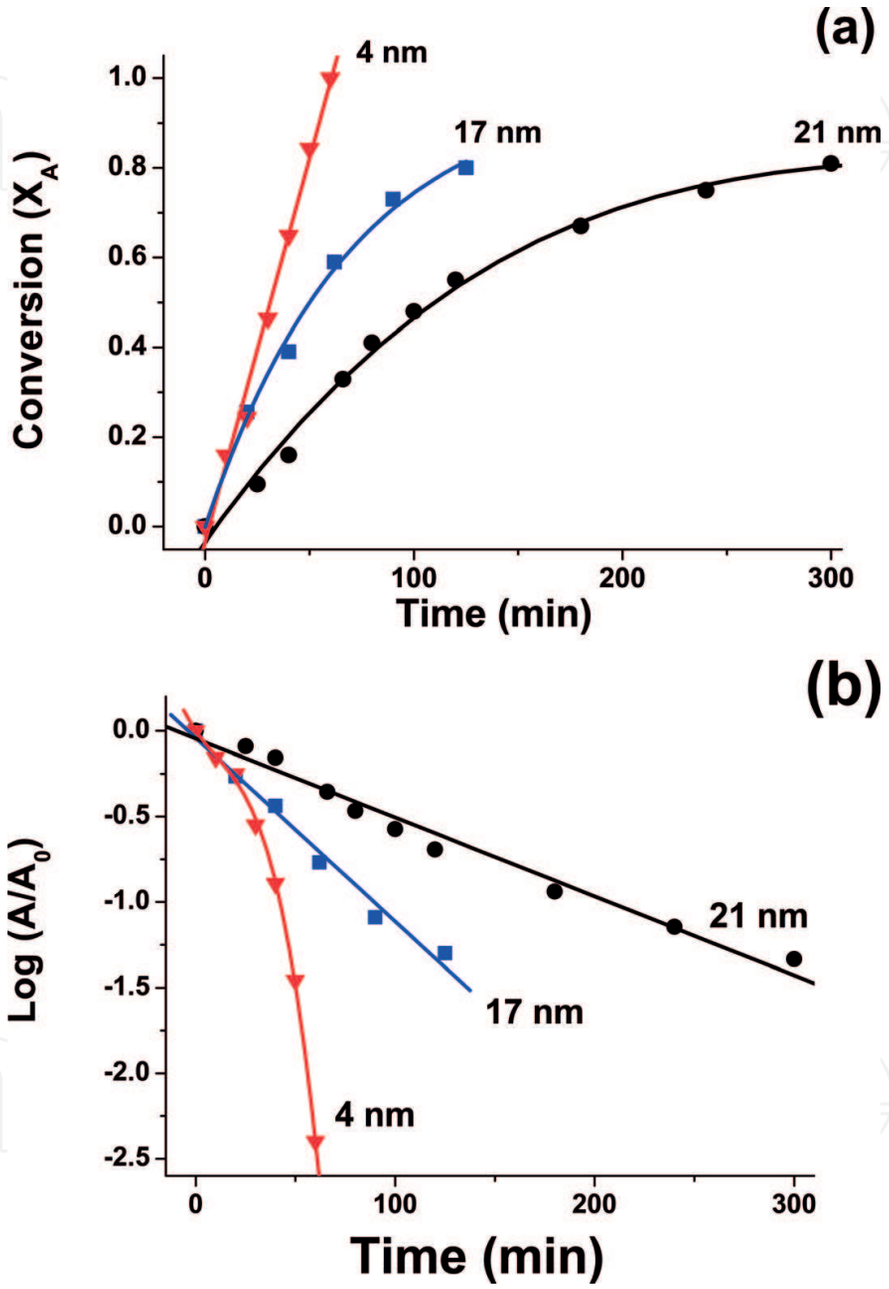

Figure 6. Glycerol consumption plots over Au/γ-Al_2O_3 catalysts prepared by various reducing agents: (a) Small gold nanoparticles (ca 4 nm) show zero-order kinetic behaviour by linearly fitting conversion as a function of reaction time; (b) big gold nanoparticles (ca 17 and 21 nm) show first-order kinetics by linearly fitting the log of concentration of glycerol as a function of reaction time. The catalysts were reduced with 5% H_2 (~4 nm), THPC (~17 nm) and PVA–citrate (~21 nm). Catalyst preparation details were outlined elsewhere [14].

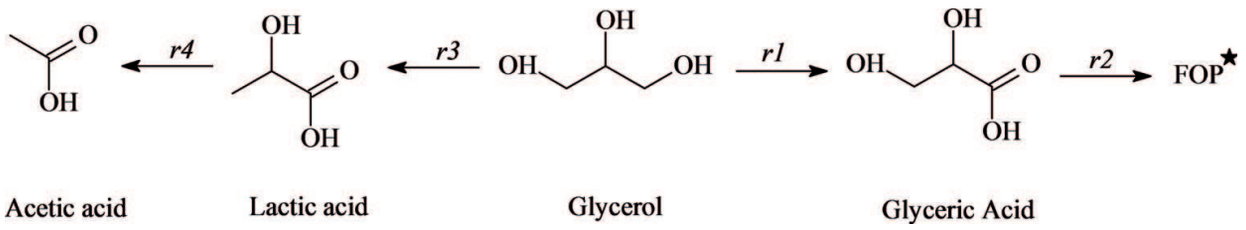

Figure 7. Reaction network used for the kinetic modelling of the glycerol oxidation. FOP* = further oxidation products (tartronic, oxalic, glycolic and formic acids).

The concentrations C_i were allocated as follows: C_1 = glycerol; C_2 = glyceric acid (GA); C_3 = FOP* (further oxidation products—FOP—were lumped together as tartronic acid, oxalic acid, glycolic acid and formic acid); C_4 = LAC and C_5 = acetic acid. The reason FOP were lumped together is that the study was only concerned with the apparent competition between the rate of formation of LAC and that of GA from glycerol and the possible effect of Lewis acidity on the rate of LAC formation. Generally, there was a good fit between the fitted pseudo-zero-order model and experiment for both tested catalysts. The results of the regression analyses of the model against experimental data showed a good fit as visually seen in **Figure 8**; the rate constants are summarised in **Table 2** for both Au/γ-Al_2O_3 and Au-MoO_3/γ-Al_2O_3, respectively. The estimated kinetic parameters were statistically significant.

From **Table 2**, one of the most intriguing results was the 'jump' in the rate of formation of LAC (k_4) over the Au-MoO_3/γ-Al_2O_3 catalyst relative to Au/γ-Al_2O_3. Indeed Eq. (10), which compares the rate of formation of LAC over the two catalysts, paints a clearer picture. It is conceivable that the extra Lewis acidity provided by Mo played a role in the promoted

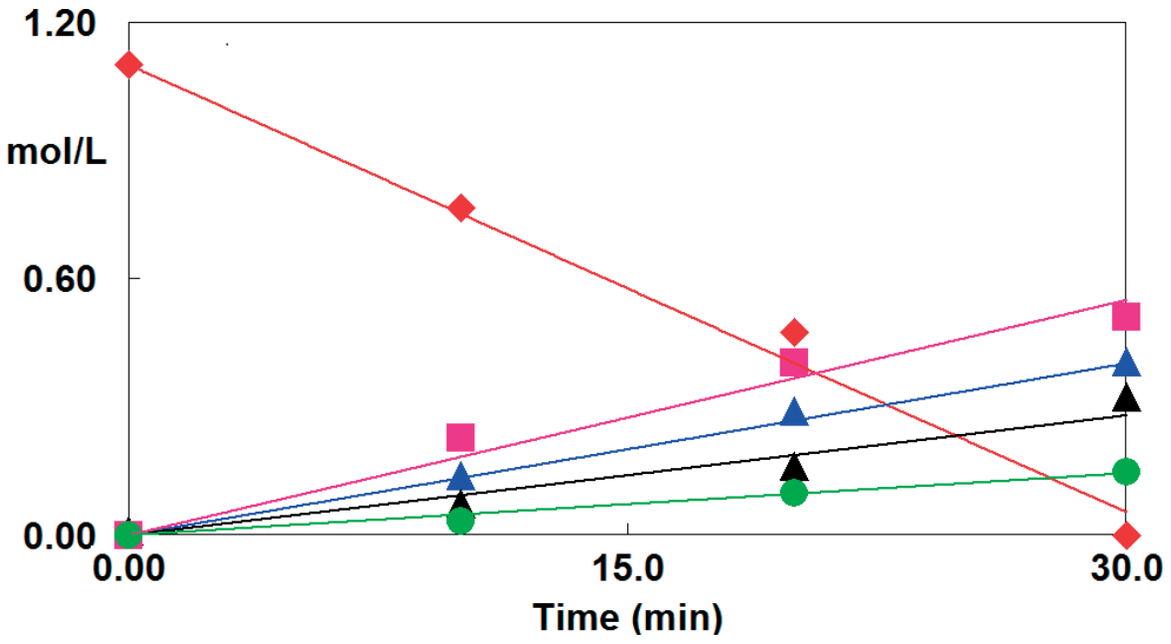

Figure 8. Comparison of computed and experimental data for glycerol oxidation assuming zero-order kinetics over Au-MoO_3/γ-Al_2O_3 (top) and Au/γ-Al_2O_3 (bottom); Glycerol (♦), glyceric acid (▲), FOP* (▲), LAC (■), acetic acid (●).

Parameter*	Catalyst					
	$Au/\gamma\text{-}Al_2O_3$			$Au/MoO_3\text{-}\gamma\text{-}Al_2O_3$		
	Value	Confidence limits		Value	Confidence limits	
k_1	0.019	0.018	0.02	0.035	0.032	0.038
k_2	0.021	0.019	0.023	0.023	0.018	0.028
k_3	0.008	0.007	0.01	0.009	0.006	0.013
k_4	0.004	0.002	0.006	0.023	0.019	0.028
k_5	0.001	0.000	0.003	0.005	0.002	0.008

*Parameter values were estimated at 95% confidence level; k = mol L^{-1} min^{-1}.

Table 2. Regression analysis of global kinetic model assuming pseudo-zero-order kinetics.

formation of LAC, as evidenced in Eq. (10) by the ratio of the rate constants of formation of LAC over the two catalysts.

$$\frac{k_{Au/MoO_3-Al_2O_3}}{k_{Au/Al_2O_3}} \cong 6 \tag{10}$$

As far as we are aware, no formation of LAC from Au-based catalysts (our work included) has been reported at 60°C except when Pd-based catalysts were used, which also gave very low turnover frequency (TOF) values (~60 h^{-1}) [10]. The TOF is the best measure of comparing catalytic performance as argued by Boudart [29]. TOF is regarded as the number of times that the overall catalytic reaction takes place per catalytic site per unit time for a fixed set of reaction conditions. Boudart has asserted that even though it may not be rigorous, a TOF measure leads to values that can be reproduced from one laboratory to another, besides catalysts of different characteristics being likened. We have therefore simplified TOF to mean the number of glycerol moles converted per the total number of moles of Au used per unit time of reaction, in hours, assuming that all the gold present in the catalyst was active. We have also assumed that the reaction occurred at constant temperature (90°C), O_2 pressure (8.5 bar), concentration (1.1 M of glycerol at t_0), and the ratio of reactants, while the extent of reaction was taken after half an hour. Thus, TOF was calculated by the equation:

$$\mathrm{TOF} = \left[\frac{(\%\,\mathrm{conversion}).(\mathrm{initial\,moles\,(glycerol)})}{100}\right].\left[\frac{1}{\mathrm{moles\,of\,Au}}\right].\left[\frac{1}{\mathrm{time\,(h)}}\right] \tag{11}$$

For example, the TOF of the Aurolite™ commercial catalyst (0.9-wt% $Au/\gamma\text{-}Al_2O_3$) after half an hour was calculated to be 4.971 h^{-1}, compared to that of $Au\text{-}MoO_3/\gamma\text{-}Al_2O_3$ catalyst (*ca* 12.800 h^{-1}). This result shows that not only does the increased acidity due the presence of Mo enhance the selectivity to LAC, but it also drives the forward conversion of glycerol. This latter point could be related to gold-support interaction effects.

3.4. Proposed role of Mo^{n+} in lactic acid formation

It is generally accepted that LAC is formed from glycerol (GLY) via the intermediates as depicted in **Figure 9** [5, 30–32]. Under the reaction conditions employed in this study, dihydroxyacetone (DHA) was formed at 60°C and could be isolated; however, at 90°C, LAC was formed instead.

It is plausible that at the latter temperature, DHA still forms but reacts further with LAC, thus assuming the role of an (unstable) intermediate. In the presence of base, DHA can form from glycerol via the isomerisation of GLA [31]. Assary et al. [33] have reported that a Lewis acid-base pair catalyses this isomerisation reaction and it is conceivable that the enhanced formation of LAC over Au-MoO_3/γ-Al_2O_3 could have been a direct consequence of the increased Lewis acid-base pair sites on the catalyst. In this section, we apply transition state theory principles [34–36] via DFT simulations to extract thermodynamic and kinetic parameters for this isomerisation reaction. Experimentally, Rasrendra et al. [37] suggested that, under catalytic conditions, GLA can be successfully isomerised to LAC. The rest of this chapter discusses the potential role played by Mo in the formation of LAC over supported bi-functional Au catalysts at low temperatures, assuming the reaction occurs according to Eq. (12).

$$GLY \xrightarrow{Au} GLA \xrightarrow{Mo-OH} LAC \tag{12}$$

DFT calculations have been done only for the second part of the reaction, since the calculations for GLY to GLA over Au have been discussed in detail elsewhere [31, 38]. The mechanism shown in **Figure 10** proposes that a crucial part of the isomerisation of GLA to LAC could be an adsorbed pyruvaldehyde (PA) molecule on the molybdenum Lewis acid site forming a five membered ring C–C–O–Mo–O. The adsorbed PA is then hydrated by a surface hydroxyl, as advanced by Kong et al. [23]. The intermediate product then undergoes a hydride shift rearrangement. Finally, a proton is then transferred from a water molecule to

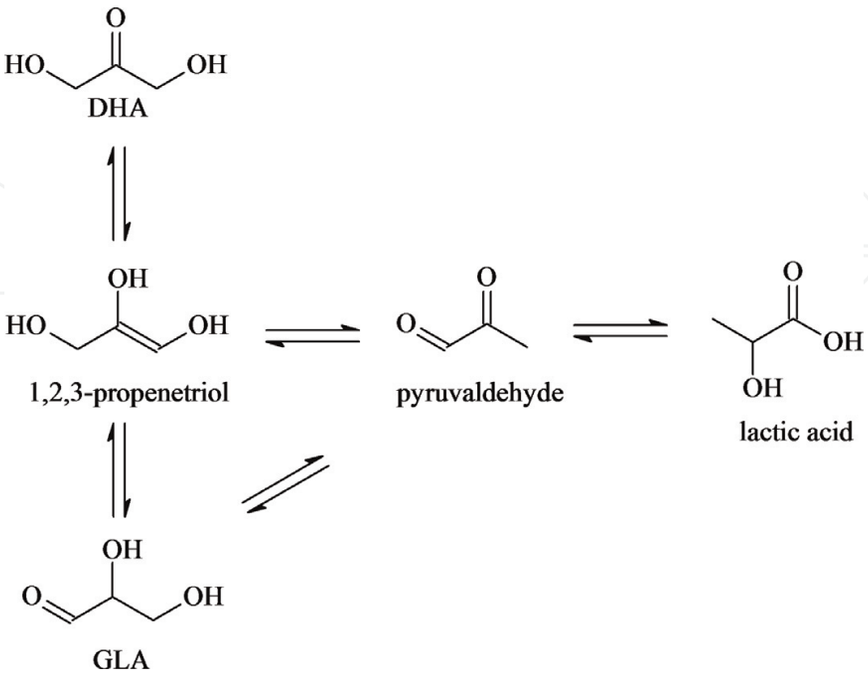

Figure 9. Proposed intermediates in the conversion of glycerol to LAC.

http://dx.doi.org/10.5772/intechopen.70485

complete the isomerisation and form a LAC molecule. Similar mechanisms have been proposed by numerous authors [5, 30, 33, 39–40], although none of these studies have modelled the mechanism at the DFT level of theory. The DFT predicted kinetic and thermodynamic parameters are summarised in **Table 3**. The reaction kinetics tool within BIOVIA Materials

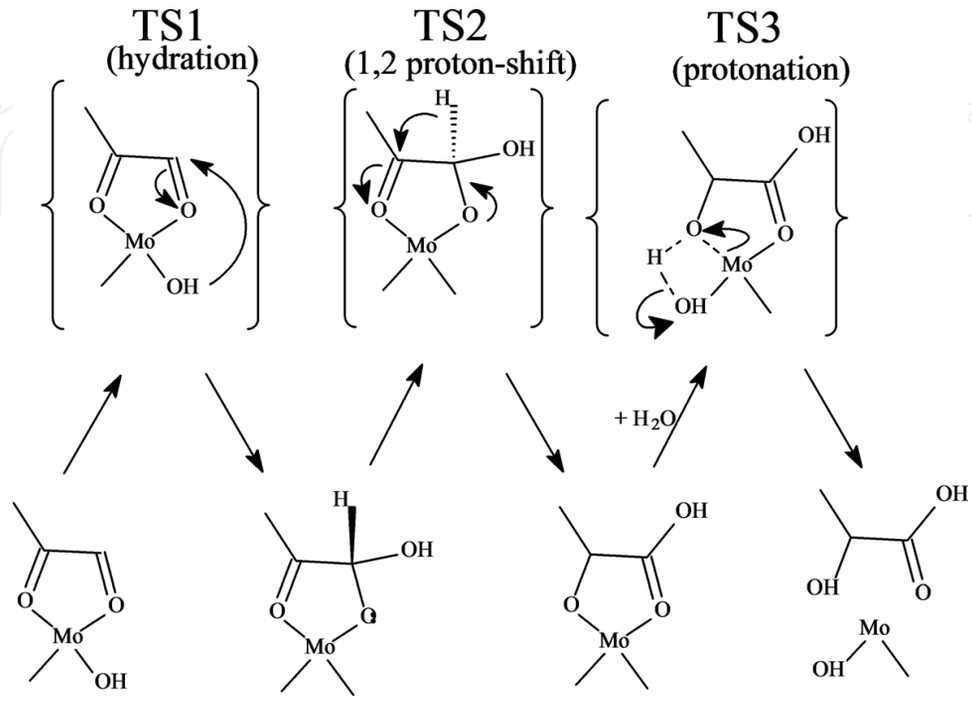

Figure 10. Possible Lewis acid-base pair dual site involved in the isomerisation of PA to LAC.

Transition state	Parameters (kJ mol^{-1})			
	Forward		Reverse	
	E_a	ΔH	E_a	ΔH
TS1 (hydration)	59.0	57.7	2.7	−57.7
TS2 (1,2 proton shift)	74.7	−57.0	131.7	57.0
TS3 (protonation)	229.7	−25.5	257.8	25.5

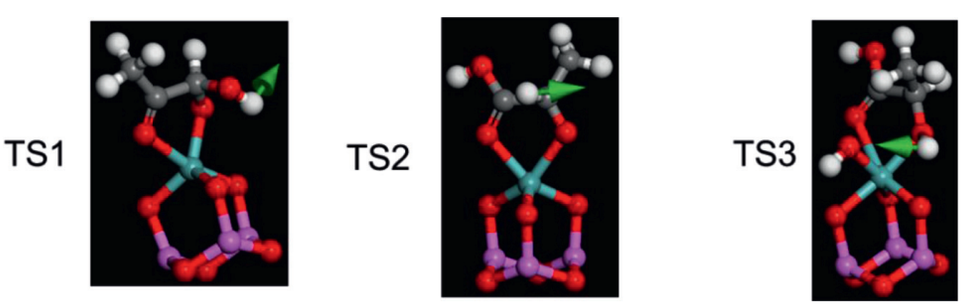

Table 3. DFT predicted kinetic and thermodynamic parameters for the Mo–OH catalysed isomerisation of PA to LAC. The direction of normal mode of vibration of the transition state is shown by the pointed arrow.

Studio 2016 was used to automate the calculations of all the parameters. Tunnelling corrections were included in all calculations. The protonation step is thermodynamically downhill, but has the highest activation barrier (229 kJ mol^{-1}) for the forward reaction as shown in the mentioned table. The magnitude of this barrier is in the order of the bond-dissociation energy of HO–H bond of a water molecule (H_2O) which requires about 268 kJ mol^{-1} at 298 K. Assuming that the reaction is controlled by kinetics, this step is the rate-limiting step. The high energy barrier for the rate-limiting step probably explains why LAC forms at 90°C under the reaction conditions employed, but none was observed at 60°C. A higher temperature is needed to overcome the barrier ($-E_a/R$) in order to get appreciable rates of the formation of the final product.

4. Conclusions

Both Au/γ-Al_2O_3 and Au-MoO_3/γ-Al_2O_3 showed zero-order kinetics under kinetic controlled glycerol oxidation. The apparent E_a of glycerol oxidation under these conditions was experimentally determined to be approximately 36 kJ mol^{-1}. Under the same reaction conditions, the presence of MoO_3 increased the formation of LAC sixfold over Au-MoO_3/γ-Al_2O_3 relative to Au/γ-Al_2O_3. A proposed DFT model suggested that protonation by an adsorbed water molecule might be the rate-limiting step in the isomerisation of PA to LAC catalysed by a Mo–OH Lewis acid-base pair.

Acknowledgements

The authors would like to thank both Mintek and Anglo-gold Ashanti through Project AuTek for granting the permission to publish this work and for financial support. In addition, we express gratitude to the South African Centre for High Performance Computing (CHPC) for their support in availing to us the infrastructure used in DFT modelling.

Author details

Thabang A. Ntho*, Pumeza Gqogqa and James L. Aluha

*Address all correspondence to: thabang.ntho@mintek.co.za

Mintek, Advanced Materials Division, Johannesburg, RSA

References

[1] Wee Y-J, Kim J-N, Ryu H-W. Biotechnological production of lactic acid and its recent applications. Food Technology Biotechnology. 2006;**44**(2):163-172

[2] Haruta M. Catalysis of gold nanoparticles deposited on metal oxides. CATTECH. 2002;**6**(3): 102-115

[3] Ketchie WC, Fang Y, Wong MS, Murayama M, Davies RJ. Influence of gold particle size on the aqueous phase oxidation of carbon monoxide and glycerol. Journal of Catalysis. 2007;**250**:94-101

[4] Ketchie WC, Murayama M, Davies RJ. Selective oxidation of glycerol over carbon supported AuPd Catalysts. Journal of Catalysis. 2007;**250**:264-273

[5] Ketchie WC, Murayama M, Davies RJ. Promotional effect of hydroxyl on the aqueous phase oxidation of carbon monoxide and glycerol over supported Au catalysts. Topics in Catalysis. 2007;**44**(1–2):307-317

[6] Wang D, Villa A, Su D, Prati L, Schlogl R. Carbon supported gold nanocatalysts: Shape effect in the selective glycerol oxidation. ChemCatChem. 2017;**5**(9):2717-2723

[7] Villa A, Wang D, Su DS, Prati L. Gold sols as catalysts for glycerol oxidation: The role of stabilizer. ChemCatChem Catalysis. 2009;**1**:510-514

[8] Demirel S, Lucas M, Lehnert K, Claus P. Use of renewables for the production of chemicals: Glycerol oxidation over carbon supported gold catalysts. Applied Catalysis B: Environmental. 2007;**70**(1-4):637-643

[9] Royker M, Case J, van Steen E. Platinum promotion of Au/Al_2O_3 catalysts for glycerol oxidation: Activity, selectivity, and deactivation. The Journal of Southern African Institute of Mining and Metallurgy. 2012;**7A**:577-581

[10] Chornaja S, Dubencov K, Kampars V, Stepanova O, Zhizhkun S, Serga V, et al. Oxidation of glycerol with oxygen in alkaline aqueous solutions in the presence of supported palladium catalysts prepared by extractive pyrolytic method. Reaction Kinetic Mechanism Catalysis. 2013;**108**:341-357

[11] Carretin S, McMorn P, Johnston P, Griffin K, Hutchings GJ. Oxidation of glycerol using supported Pt, Pd and Au catalysts. Physical Chemistry Chemical Physics. 2003;**5**:1329-1336

[12] Stobbe-Kreemers AW, Vanleerdam GCV, Jacobs JP, Brogersma HH, Scholten JJF. Characterization of γ-alumina-supported vanadium oxide monolayers. Journal of Catalysis. 1995;**152**:130-136

[13] Raubenheimer HG, Cronje S. Progress in Chemistry, Biochemistry and Biotechnology. Chichester: John Wiley & Sons; 1999. 573-576

[14] Ntho T, Aluha J, Gqogqa P, Raphulu M, Pattrick G. $Au/\gamma\text{-}Al_2O_3$ catalysts for glycerol oxidation: The effect of support acidity and gold particle size. Reaction Kinetic Mechanism and Catalysis. 2013;**109**(1):133-148

[15] Belohlav Z, Zamostny P, Kluson P, Volf J. Application of random-search algorithm for regression analysis of catalytic hydrogenations. Canadian Journal of Chemical Engineering. 1997;**75**:735-742

[16] Zamostny P, Belohlav Z. A software for regression analysis. Computers and Chemistry. 1999;**23**:479-485

[17] Delley B. An all-electron numerical method for solving the local density functional for polyatomic molecules. The Journal of Chemical Physics. 1990;**92**:508-517

[18] Delley B. From molecules to solids with the DMol3 approach. Journal of Chemical Physics. 2000;**113**:7756-7764

[19] Govind N, Petersen MM, Fitzgerald G, King-Smith D, Andzelm J. A generalized synchronous transit method for transition state location. Computational Materials Science. 2003;**28**(2):250-258

[20] Sheppard D, Terrell R, Henkelman G. Optimization methods for finding minimum energy paths. The Journal of Chemical Physics. 2008;**128**:134106-134116

[21] Handzlik J, Ogonowski J. Theoretical study on ethene metathesis proceeding on Mo^{VI} and Mo^{IV} methylidene centres of heterogeneous molybdena-alumina catalyst. Journal of Molecular Catalysis A: Chemical. 2001;**175**:215-225

[22] Song X, Liu G, Yu J, Rodrigues AE. Density functional theoretical study of water molecular adsorption on surface of MoO_3 with the cluster model. Journal of Molecular Structure (Theochem). 2004;**684**:81-85

[23] Kong L, Li G, Wang H, He W, Ling F. Hydrothermal catalytic conversion of biomass for lactic acid production. Journal of Chemical Technology and Biotechnology. 2008;**83**:383-388

[24] Lianecki M, Malecka-Grycz M, Domka F. Water-gas shift reaction over sulfided molybdenum catalysts I. Alumina, titania and zirconia-supported catalysts. Applied Catalysis A: General. 2000;**196**:293-303

[25] Heracleous E, Lemonidou AA, Lercher JA. Mechanistic features of the ethane oxidative dehydrogenation by in situ FTIR spectroscopy over a MoO_3/Al_2O_3 catalyst. Applied Catalysis A: General. 2004;**264**:73-80

[26] Gong J, Ma X, Wang S, Yang X, Wang G, Wen S. Effect of Mo content in $MoO_3/\text{-}\gamma\text{-}Al_2O_3$ on the catalytic activity for trans-esterification of dimethyl oxalate with phenol. Reaction Kinetics and Catalysis Letters. 2004;**83**(1):113-120

[27] Wörz N, Brandner A, Claus P. Platinum-bismuth catalyzed oxidation of glycerol: Kinetics and the origin of selective deactivation. Journal of Physical Chemistry C. 2010;**114**:1164-1172

[28] Demirel S, Lucas M, Warna J, Salmi T, Murzin D, Claus P. Reaction kinetics and modelling of the gold catalysed glycerol oxidation. Topics in Catalysis. 2007;**44**(1-2):299-305

[29] Boudart M. Turnover rates in heterogeneous catalysis. Chemical Reviews. 1995;**95**:661-666

[30] Shen Y, Zhang S, Li H, Ren Y, Liu H. Efficient synthesis of lactic acid by aerobic oxidation of glycerol on Au-Pt/TiO_2 catalysts. Chemistry – A European Journal. 2010;**16**:7368-7371

[31] Zope BN, Hibbits DD, Neurock M, Davis RJ. Reactivity of the gold/water interface during selective oxidation catalysis. Science. 2010;**330**:74-78

[32] Román-Leshkov Y, Davis ME. Activation of carbonyl containing molecules with solid Lewis acids in aqueous media. ACS Catalysis. 2011;**1**:1566-1580

[33] Assary RS, Curtiss LA. Theoretical study of 1, 2-hydride shift associated with the isomerisation of glyceraldehyde to dihydroxy acetone by Lewis acid active site models. Journal of Physical Chemistry A. 2011;**115**:8754-8760

[34] Evans MG, Polanyi M. Some applications of the transition state method to the calculation of reaction velocities, especially in solution. Transactions of the Faraday Society. 1935;**31**:875-894

[35] Eyring H. The activated complex in chemical reactions. Journal of Chemical Physics. 1935;**3**:107-116

[36] Geng Z, Zhang M, Yu Y. Theoretical investigation on pyrolysis mechanism of glycerol. Fuel. 2012;**93**:92-98

[37] Rasrendra CB, Marketihartha IGBN, Adisasmito S, Heeres HJ. Green chemicals from d-glucose: Systematic studies on catalytic effects of inorganic salts on the chemo-selectivity and yield in aqueous solutions. Topics in Catalysis. 2010;**53**(15-18):1241-1247

[38] Shang C, Liu Z-P. Origin and activity of gold nanoparticles as aerobic oxidation catalysts in aqueous solution. Journal of American Chemical Society. 2011;**133**:9938-9947

[39] West RM, Holm MS, Saravanamurugan S, Xiong J, Beversdorf Z, Christensen CH. Zeolite H-USY for the production of lactic acid and methyl lactate from C-3 sugars. Journal of Catalysis. 2010;**269**:122-130

[40] Rasrendra CB, Fachri BA, Marketihartha IGBN, Adisasmito S, Heers HJ. Catalyic conversion of dihydroxyacetone to lactic acid using metal salts in water. Journal of Sustainable Chemistry. 2011;**4**:768-777

IntechOpen